PROCEEDINGS OF SCIENCE

Studying the (α, p)-process in X-ray Bursts using Radioactive Ion Beams

Catherine M. Deibel*
Joint Institute for Nuclear Astrophysics, Michigan State University, East Lansing, MI 48824, USA
Physics Division, Argonne National Laboratory, Argonne, IL 60439, USA

Martin Alcorta, Peter F. Bertone, Jason A. Clark, John Greene, Calem R. Hoffman, Cheng Lie Jiang, Benjamin P. Kay, Hye-Young Lee, Richard C. Pardo, K. Ernst Rehm, Andrew Rogers, Claudio Ugalde, Gary Zinkann
Physics Division, Argonne National Laboratory, Argonne, IL 60439, USA

Shadi Bedoor, Dinesh V. Shetty, Alan H. Wuosmaa
Physics Department, Western Michigan University, Kalamazoo, MI 49008, USA

Jonathan C. Lighthall, Scott T. Marley
Physics Department, Western Michigan University, Kalamazoo, MI 49008, USA
Physics Division, Argonne National Laboratory, Argonne, IL 60439, USA

Nidhi R. Patel
Department of Physics, Colorado School of Mines, Golden, CO 80401, USA
Physics Division, Argonne National Laboratory, Argonne, IL 60439, USA

Juan Manuel Figueira
Laboratorio Tandar, B1650KNA San Martin, Buenos Aires, Argentina

Michael Paul
Racah Institute of Physics, Hebrew University, Jerusalem, Israel 91904

PROCEEDINGS OF SCIENCE

In type I X-Ray Bursts (XRBs) the nuclear flow is driven towards the proton-drip line by the triple-α reaction, the (α,p)-process, and the rp-process. Along the nucleosynthetic path, the reaction flow can be stopped at so-called waiting-point nuclei. The low $Q_{p\gamma}$ value of a waiting-point nucleus leads to (p,γ)-(γ,p) equilibrium causing the flow to stall and await a β decay. However, if the temperature is high enough the competing (α,p) reaction can bypass the waiting point. This can have significant effects on the final elemental abundances, energy output, and observables such as double-peaked luminosity profiles. In the intermediate mass region ^{22}Mg, ^{26}Si, ^{30}S, and ^{34}Ar have been identified as possible candidates for waiting-point nuclei in XRBs.

A method to study the (α,p)-process on intermediate mass waiting-point nuclei has been developed whereby the time-inverse reaction is studied in inverse kinematics using radioactive ion beams produced by the in-flight method at the ATLAS facility at Argonne National Laboratory. The three reactions $p(^{29}\mathrm{P},^{26}\mathrm{Si})\alpha$, $p(^{33}\mathrm{Cl},^{30}\mathrm{S})\alpha$, and $p(^{37}\mathrm{K},^{34}\mathrm{Ar})\alpha$ have been studied for the first time to determine cross sections for $^{26}\mathrm{Si}(\alpha,p)^{29}\mathrm{P}$, $^{30}\mathrm{S}(\alpha,p)^{33}\mathrm{Cl}$, and $^{34}\mathrm{Ar}(\alpha,p)^{37}\mathrm{K}$, respectively. The results and future plans will be discussed.

11th Symposium on Nuclei in the Cosmos, NIC XI
July 19-23, 2010
Heidelberg, Germany

---

[*] Speaker.

1. Introduction

Type I X-Ray Bursts (XRBs) occur in binary star systems where a neutron star accretes matter from its companion, a main sequence star. As the accreted hydrogen-rich matter builds up on the surface of the neutron star the temperature and the pressure increase and a thermonuclear runaway occurs reaching peak temperatures of $T_{peak} = 1-2$ GK. These bursts typically last for $10-100$ s with recurrence times on the order of a few hours to several days [1]. As the reaction flow proceeds through the triple-α reaction, (α,p)-process, and rp-process on the proton-rich side of stability it can be stalled at so-called waiting-point nuclei. Specifically, this may occur in the A $= 20-40$ mass regime when a (p,γ)-(γ,p) equilibrium is reached at a nucleus with a low $Q_{p\gamma}$ value, whose β^+-decay half life is on the order of seconds. Candidates for these intermediate mass waiting points are ^{22}Mg, ^{26}Si, ^{30}S, and ^{34}Ar [2]. The half-lives of these nuclei are significantly long on XRB time scales and may affect the nucleosynthetic path; however, at XRB temperatures (α,p) reactions on these nuclei may be fast enough to break out of these waiting points. Thus the ^{26}Si(α,p), ^{30}S(α,p), and ^{34}Ar(α,p) reactions are thought to be the most important reactions in the (α,p)-process in XRBs [2]. The interplay between the (p,γ)-(γ,p) equilibrium, (α,p) breakout reaction, and β^+ decay at a waiting point helps to determine the nucleosynthetic flow and may be directly observable in the double-peaked luminosity profiles of some XRBs [3].

As neutron stars are very dense, compact objects, the elements created during an XRB are not ejected into the interstellar medium, but rather are added to the neutron star's crust and become seeds for the reactions in subsequent XRBs. In order to understand these evolving systems it is necessary to know the nuclear masses, β-decay half lives, and reaction rates involved in XRB nucleosynthesis so that the final elemental abundances and the energy output of XRBs can be accurately modeled. Thousands of reaction rates have been used in these models, although recent sensitivity studies [4] have shown that relatively few of those have significant effects on elemental abundances and energy output produced; ^{30}S$(\alpha,p)^{33}$Cl being among them.

Unfortunately, most of the reaction rates used in XRB models are theoretical as the reactions involved tend to be close to the proton-drip line and therefore experimentally inaccessible. However, there are some reactions which can be studied at current facilities. Three of the proposed (α,p)-process waiting points, ^{26}Si, ^{30}S, and ^{34}Ar, have been studied in inverse kinematics using radioactive ion beams produced at the ATLAS facility at Argonne National Laboratory to measure the time-inverse reactions $p(^{29}\text{P},^{26}\text{Si})\alpha$, $p(^{33}\text{Cl},^{30}\text{S})\alpha$, and $p(^{37}\text{K},^{34}\text{Ar})\alpha$.

2. Experiment

Radioactive ion beams were produced using the in-flight method at ATLAS [5]. Stable beams of ^{28}Si, ^{32}S, and ^{36}Ar at energies of approximately $320-325$ MeV were incident on a LN_2-cooled gas cell filled with 1.4 atm of deuterium gas to produce ^{29}P, ^{33}Cl, and ^{37}K, respectively, via the (d,n) reaction. The reaction products were then refocused and separated from the residual stable beam before reaching the experimental area. Typical beam intensities achieved, using approximately 400 enA of primary beam, ranged from $\sim 1-4\times10^4$ particles/s for the radioactive ion beams of ^{29}P, ^{33}Cl, and ^{37}K at energies of 280 MeV, 250 MeV, and 275 MeV, respectively.

To measure cross sections of these reactions at a range of energies the beam energy needs to be changed, which, for stable ion beams, is typically done by accelerating the beam to lower energies. However, decreasing the energy of the primary beam and retuning the radioactive ion beam would have been prohibitively time consuming due to the complex nature of making these beams with the in-flight method. Energy changes were therefore achieved by passing the radioactive ion beam through Au degrader foils, which lowered the beam energy in steps of approximately 20 MeV, as measured in the spectrograph. Using this method ^{33}Cl beams of 250, 229, and 208 MeV and the ^{37}K beams of approximately 275 MeV, 255 MeV, and 235 MeV were produced.

In each reaction the radioactive ion beam was incident on a 650 μg/cm^2 CH$_2$ target. The α particles produced in the (p,α) reactions were detected in an annular double-sided Si detector (DSSD) segmented into 16 rings in θ_{lab}, which covered the angles $\theta_{lab} = 8^\circ - 24^\circ$ for the $p(^{33}\mathrm{Cl},^{30}\mathrm{S})\alpha$ and $p(^{37}\mathrm{K},^{34}\mathrm{Ar})\alpha$ reactions and $\theta_{lab} = 6^\circ - 19^\circ$ for the $p(^{29}\mathrm{P},^{26}\mathrm{Si})\alpha$ reaction.

The heavier reaction products were momentum analyzed by an Enge split-pole spectrograph to separate the residual nuclei of interest from beam contaminants. In order to focus the particles of interest from all the charge states produced onto the focal plane, the spectrograph was run in gas-filled mode and was filled with approximately 15 torr of N$_2$ gas for the highest energy beams (the pressure was lowered for the lower energy beams). The charge exchange reactions between the ions and the gas led to a collapse of the charge state distribution into a mean charge state so that all the residual nuclei could be detected at the focal plane. A parallel grid avalanche counter (PGAC) and ionization chamber detected the products at the focal plane of the spectrograph and measured their magnetic rigidity, energy loss, and time of flight. Unfortunately, the heavy recoils associated with the low-energy α branch had the same magnetic rigidity as the contaminant beam and had to be blocked to avoid prohibitively high counting rates. Thus only those recoils associated with the high-energy α branch were detected.

3. Results and Conclusion

By detecting the α particles in coincidence with the heavier reaction products of interest the yields from the $p(^{29}\mathrm{P},^{26}\mathrm{Si})\alpha$, $p(^{33}\mathrm{Cl},^{30}\mathrm{S})\alpha$, and $p(^{37}\mathrm{K},^{34}\mathrm{Ar})\alpha$ reactions were measured. Some of the background was eliminated by gating around the particle group of interest detected at the focal plane. A typical kinematic curve of the θ_{lab} dependence on the α-particle energy for the $p(^{33}\mathrm{Cl},^{30}\mathrm{S})\alpha$ reaction is shown in Figure 1 and is in good agreement with Monte Carlo simulations. By correcting the α-particle yield for the various geometrical efficiencies associated with the detector setup and for the lower energy α branch, and normalizing to the target thickness and beam current, the cross sections for the $p(^{33}\mathrm{Cl},^{30}\mathrm{S})\alpha$ and $p(^{37}\mathrm{K},^{34}\mathrm{Ar})\alpha$ reactions were measured at three different energies. The $p(^{29}\mathrm{P},^{26}\mathrm{Si})\alpha$ reaction has so far only been measured at 280 MeV; however, measurements at lower energies are planned. Preliminary results show that the cross sections are typically a factor of four or more larger than the NONSMOKER theoretical cross sections [6, 7, 8] and on the order of $1-10$ mb for the $p(^{33}\mathrm{Cl},^{30}\mathrm{S})\alpha$ measurement.

These increases in cross sections imply that breakout from these waiting point nuclei via the (α,p) reaction is more likely to occur. However, due to the extremely low cross sections of these reactions, and the low intensity of radioactive ion beams available, the cross sections measured here are at energies above the astrophysically relevant regime. While the cross sections for the

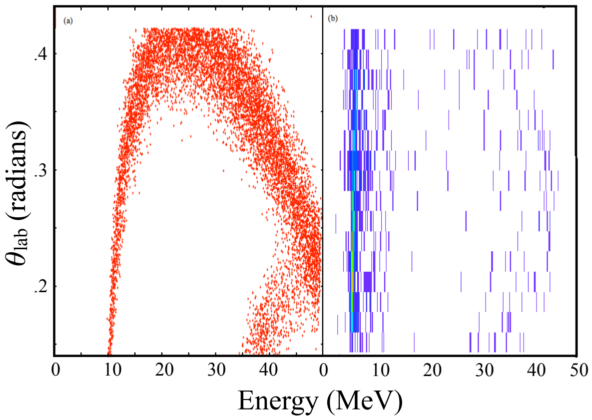

Figure 1: θ_{lab} (degrees) as a function of α energy (MeV) for the $p(^{33}\mathrm{Cl},^{30}\mathrm{S})\alpha$ reaction with a 250 MeV ^{33}Cl beam (a) simulated by a Monte Carlo simulation and (b) experimentally measured by the DSSD. Note that the DSSD only measures the high-energy α branch (see text for details); the counts at lower energies are from proton inelastic scattering. On the order of 100 counts are detected in the high-energy α branch.

$p(^{33}\mathrm{Cl},^{30}\mathrm{S})\alpha$ reaction were measured at energies of $6-7.5$ MeV in the center of mass, the astrophysically relevant energy regime is 3.5 - 4.4 MeV. The energy range measured for the other reactions discussed herein is similarly much higher than the astrophysically relevant region. In order to determine how these reaction rates affect the nucleosynthesis in XRBs, measurements at lower energies are needed. Furthermore, these reactions should ideally be measured in the forward direction using radioactive ion beams incident on an α target. Such experiments using the new HELIOS device at ATLAS [9] are currently being examined.

References

[1] H. Schatz and K. E. Rehm, Nucl. Phys. **A777**, 601 (2006).

[2] J. L. Fisker, H. Schatz, and F.-K. Thielemann, Astrophys. J. Supp. Ser. **174**, 261 (2008).

[3] J. L. Fisker, F. K. Thielemann, and M. Wiescher, Astrophys. J. Lett. **608**, 61 (2004).

[4] A. Parikh, J. José, F. Moreno, and C. Iliadis, Astrophys. J. Supp. Ser. **178**, 110 (2008).

[5] B. Harss *et al.*, Phys. Rev. Lett. **82**, 3964 (1999).

[6] T. Rauscher and F.-K Thielemann, At. Data Nucl. Data Tables **75**, 1 (2000).

[7] T. Rauscher and F.-K Thielemann, At. Data Nucl. Data Tables **79**, 47 (2001).

[8] *NON-SMOKER code, http://nucastro.org/nonsmoker.html*

[9] J. C. Lighthall *et al.*, Nucl. Instrum. Methods **A622**, 97 (2010).

Acknowledgments

This work has been supported by JINA grant No. PHY0822648 and U.S. DOE contract DE-AC02-06CH11357. We would also like to thank the ATLAS operations staff for making this study possible.